Computer Methods in Applied Mechanics and Engineering 108 (1993) 53–71
North-Holland

CMA 418

Thermal stress analysis of axisymmetric bodies via the boundary element method

Manoj B. Chopra and Gary F. Dargush
Department of Civil Engineering, State University of New York at Buffalo, Buffalo, NY 14260, USA

Received 7 February 1992

A time dependent boundary element method (BEM) for evaluating thermal stresses in an axisymmetric thermoelastic body has been developed. Previous BEM work on axisymmetric thermoelasticity is extended to permit the calculation of stresses at both boundary and interior points. However, the new formulation still requires only surface discretization and is capable of very accurate evaluation of stress. The boundary displacement integral equation is successively differentiated to obtain the corresponding stress and strain integral equations. Explicit expressions for the steady-state axisymmetric fundamental solutions are derived in this process. The non-steady components of the integrands are obtained directly from the corresponding three-dimensional counterparts. The numerical implementation of this formulation is carried out within a general purpose BEM computer code and several numerical examples are presented to illustrate the accuracy and applicability of the method.

1. Introduction

The boundary element method has been applied to the field of thermomechanics with considerable success. The first formulations for uncoupled steady-state thermoelasticity were presented by Rizzo and Shippy [1] in three dimensions and by Cruse et al. [2] in axisymmetry. In both these efforts, the temperature gradients were treated in the manner of body forces and the resulting volume integral was converted to surface integrals by utilizing the properties of an assumed steady-state temperature distribution. Subsequently, an axisymmetric thermoelastic formulation with higher order elements was presented by Bakr and Fenner [3]. Explicit fundamental solutions for the coupling terms were provided in this work, which were later used by Bakr et al. [4] to solve a number of illustrative examples.

In the field of non-steady BEM for this class of problems, the first development may be attributed to Banerjee and Butterfield [5] who proposed a volume-based procedure for dealing with the resulting body forces, in the analogous field of soil consolidation. Recent advances in transient thermoelasticity have been made by Masinda [6] in three dimensions and Tanaka et al. [7] and Sharp and Crouch [8] in two dimensions. All of these efforts resort to a volume integration approach and are, thus, not true BEM.

Recently, Dargush and Banerjee [9–11] have presented general, time-domain quasistatic BEM formulations for two- and three-dimensional analyses, wherein only surface discretization is required. Subsequently, a boundary-only axisymmetric formulation was developed by Dargush and Banerjee [12] for quasistatic thermal analysis. This formulation, however, was restricted only to surface computations. The present paper aims to extend this formulation to enable the computation of thermal stress at any point on or within a thermoelastic body. It may be noted that the advantage of surface-only discretization is preserved.

Starting in the next section with the governing differential equations for uncoupled quasistatic thermoelasticity in three dimensions, the process of obtaining the integral formulations for pure axisymmetry via suitable transformations is discussed in brief. As shown in the previous work, the fundamental solutions are decomposed into the steady and transient components. This is followed by progressive differentiation of the boundary displacement integral equation to obtain the integral

Correspondence to: Professor Gary F. Dargush, Department of Civil Engineering, State University of New York at Buffalo, 212 Ketter Hall, Buffalo, NY 14260, USA.

0045-7825/93/$06.00

3. Integral formulations for axisymmetry

In order to model an axisymmetric geometry, adopting a cylindrical coordinate system (r, θ, z) becomes more convenient. In this system, the surface S is formed only by a generator C lying in the r–z plane as shown in Fig. 1. The generalized coordinates, u_β and t_β, can now be transformed into the cylindrical system. By considering only purely axisymmetric behavior, the circumferential degree of freedom is eliminated and $u_\theta = 0$, $t_\theta = 0$. Next, the kernel functions are integrated from 0 to 2π in the circumferential direction. The steady state kernels, $G_{\beta\alpha}$ and $F_{\beta\alpha}$, can be integrated analytically in terms of elliptic integrals while the transient components require numerical treatment. Thus, upon transformation and integration, the boundary integral equation becomes [12]

$$\bar{c}_{\beta\alpha}(\xi)\bar{u}_\beta(\xi,\tau) = \int_C [\hat{G}_{\beta\alpha}(X;\xi)\bar{t}_\beta(X,\tau) - \hat{F}_{\beta\alpha}(X;\xi)\bar{u}_\beta(X,\tau)]\, \mathrm{d}C + \int_C \int_0^{2\pi} [\bar{g}^{\mathrm{tr}}_{\beta\alpha}(X;\xi,\tau) * \bar{t}_\beta(X) - \bar{f}^{\mathrm{tr}}_{\beta\alpha}(X;\xi,\tau) * \bar{u}_\beta(X)]\, \mathrm{d}\theta\, \mathrm{d}C\,, \tag{6}$$

where

$$\bar{u}_\alpha = T_{\beta\alpha} u_\beta = \{u_r \quad u_z \quad T\}^{\mathrm{t}}\,, \qquad \bar{t}_\alpha = T_{\beta\alpha} t_\beta = \{t_r \quad t_z \quad q\}^{\mathrm{t}}\,, \tag{7a,b}$$

where $T_{\beta\alpha}$ is the transformation tensor and the kernel functions are suitably transformed into the cylindrical system as described in [12]. By definition, the integrated steady state kernels are given by

$$\hat{G}_{\beta\alpha} = \int_0^{2\pi} \bar{G}_{\beta\alpha}\, \mathrm{d}\theta\,, \qquad \hat{F}_{\beta\alpha} = \int_0^{2\pi} \bar{F}_{\beta\alpha}\, \mathrm{d}\theta\,, \tag{8a,b}$$

where

$$\bar{G}_{\beta\alpha} = \tilde{T}_{\gamma\beta} G_{\gamma\delta} T_{\delta\alpha} r(X)\,, \qquad \bar{F}_{\beta\alpha} = \tilde{T}_{\gamma\beta} F_{\gamma\delta} T_{\delta\alpha} r(X)\,, \tag{9a,b}$$

$$\bar{g}^{\mathrm{tr}}_{\beta\alpha} = \tilde{T}_{\gamma\beta} g^{\mathrm{tr}}_{\gamma\delta} T_{\delta\alpha} r(X)\,, \qquad \bar{f}^{\mathrm{tr}}_{\beta\alpha} = \tilde{T}_{\gamma\beta} f^{\mathrm{tr}}_{\gamma\delta} T_{\delta\alpha} r(X)\,, \tag{9c,d}$$

$$\bar{c}_{\beta\alpha} = \tilde{T}_{\gamma\beta} c_{\gamma\delta} T_{\delta\alpha}\,, \tag{9e}$$

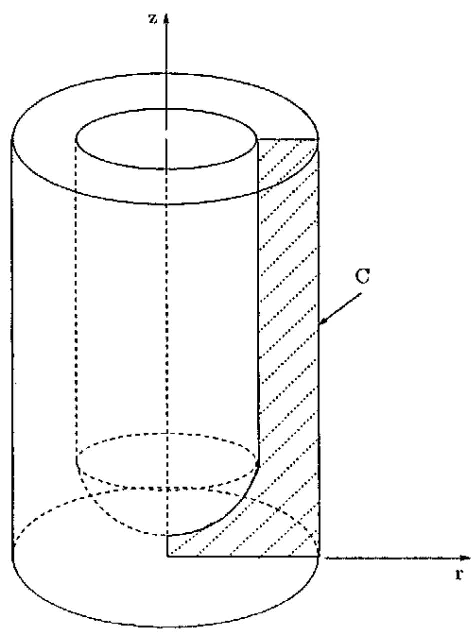

Fig. 1. Axisymmetric geometry.

where the constants c_1 and c_2 are given by

$$c_1 = \frac{E(1-\nu)}{(1+\nu)(1-2\nu)}, \qquad c_2 = \frac{E\nu}{(1+\nu)(1-2\nu)}. \tag{15a,b}$$

Explicit expressions for all the derivative terms in (13) and (14), and the steady-state axisymmetric kernels for interior stress are presented in Appendix A. The transient kernels are detailed at a later stage in the formulation. Equations (6), (10) and (12) are all exact statements with no approximations made. Therefore, in principle, if equations (6) are written for every point on the boundary starting from time zero to the present time and solved simultaneously, exact solutions to the desired boundary value problem can be obtained. In reality, however, the analysis must be restricted to a finite number of equations at some discrete time intervals. This is done by using discretization within a numerical algorithm as discussed in the next section.

4. Numerical implementation

The application of the integral equations for boundary displacements and interior stresses to problems of practical engineering interest requires discretization in both time and space. Dargush and Banerjee [12] provide an insight into the numerical implementation schemes for the axisymmetric analysis from the viewpoint of boundary displacements. The present discussion is confined to the different features of the numerical algorithm for the evaluation of stresses in the interior.

For the temporal discretization, the time interval from zero to t can be divided into N equal increments of duration Δt without any precision loss. Thus, the convolution integrals in (12) with limits from zero to t can be represented as a sum of N integrals. By assuming that the primary variables, $\bar{u}_\beta$ and $\bar{t}_\beta$ remain constant within each time increment Δt, these variables can be brought outside the integrals in (12) and the stress equation may be written, for the Nth time increment as

$$\begin{aligned}\bar{\sigma}_{ij}^{N}(\xi) = &\int_C [\hat{G}^{\sigma}_{\beta ij}(X;\xi)\bar{t}^{N}_{\beta}(X) - \hat{F}^{\sigma}_{\beta ij}(X;\xi)\bar{u}^{N}_{\beta}(X)]\,\mathrm{d}C \\ &+ \sum_{n=1}^{N}\left\{\int_C [\hat{G}^{\sigma;N-n+1}_{\beta ij}(X;\xi)\bar{t}^{n}_{\beta}(X) - \hat{F}^{\sigma;N-n+1}_{\beta ij}(X;\xi)\bar{u}^{n}_{\beta}(X)]\,\mathrm{d}C\right\},\end{aligned} \tag{16}$$

where the interior stress transient kernels are

$$\hat{G}^{\sigma;N-n+1}_{\beta ij} = \int_0^{2\pi} \bar{G}^{\sigma;N-n+1}_{\beta ij}\,\mathrm{d}\theta, \qquad \hat{F}^{\sigma;N-n+1}_{\beta ij} = \int_0^{2\pi} \bar{F}^{\sigma;N-n+1}_{\beta ij}\,\mathrm{d}\theta, \tag{17a,b}$$

with

$$\bar{G}^{\sigma;N-n+1}_{\beta ij}(X;\xi) = \int_{(n-1)\Delta t}^{n\,\Delta t} {}^{\mathrm{tr}}\bar{g}^{\sigma}_{\beta ij}(X,t;\xi,\tau)\,\mathrm{d}\tau, \tag{18a}$$

$$\bar{F}^{\sigma;N-n+1}_{\beta ij}(X;\xi) = \int_{(n-1)\Delta t}^{n\,\Delta t} {}^{\mathrm{tr}}\bar{f}^{\sigma}_{\beta ij}(X,t;\xi,\tau)\,\mathrm{d}\tau. \tag{18b}$$

Alternatively, the axisymmetric stress kernels may be obtained directly from the three-dimensional kernels by suitable transformation as follows:

$$\bar{G}^{\sigma;N-n+1}_{\beta ij}(X;\xi) = G^{\sigma;N-n+1}_{\gamma ij} T_{\gamma\beta} r(X), \tag{19a}$$

$$\bar{F}^{\sigma;N-n+1}_{\beta ij}(X;\xi) = F^{\sigma;N-n+1}_{\gamma ij} T_{\gamma\beta} r(X). \tag{19b}$$

The time integration of the three-dimensional kernels is performed analytically and the resulting transient stress kernels are provided in Appendix A. However, similar to the case of the boundary equation [12], the circumferential integration in (17) cannot be done in closed form and requires the use of Gaussian quadrature formulae. Self-adaptive integration, with subsegmentation and higher order Gaussian rules, is employed in this circumferential integration scheme.

Having discussed a piecewise constant time marching scheme to discretize the time interval for the solution, the next step is the discretization of the director C in the r–z plane to enable numerical state whereas the outer face is held at zero. The following material properties are selected to represent the cylinder:

$$E = 1.0\,, \qquad \nu = 0.3\,, \qquad \alpha = 1.0\,, \qquad k = 1.0\,.$$

The axisymmetric BEM mesh for this problem is shown in Fig. 2. It consists of ten quadratic boundary elements containing twenty-one nodes. This discretization was found to be sufficient to yield very accurate results. Conditions of symmetry are imposed at $Z = 0$ and no elements are required at that surface. However, a number of interior (sampling) points are placed on the plane of symmetry, as shown in Fig. 2, to evaluate the interior quantities such as temperature and stress. These quantities are then used for comparison with an analytical solution to this problem to establish the validity of the analysis.

The analytical solution is presented by Timoshenko and Goodier [18] for the temperature distribution as well as the thermal stresses at steady state. If a is the inner radius, b the outer radius and T_i is the temperature of the inner surface, with the outer held at zero, then the radial variation of temperature is given by

$$T(r) = \frac{T_i}{\log(b/a)} \log \frac{b}{r}\,,$$

and the stresses are given by

$$\sigma_{rr} = \frac{\alpha E T_i}{2(1-\nu)\log(b/a)} \left[-\log\frac{b}{r} - \frac{a^2}{(b^2-a^2)}\left(1 - \frac{b^2}{r^2}\right)\log\frac{b}{a} \right]$$

$$\sigma_{\theta\theta} = \frac{\alpha E T_i}{2(1-\nu)\log(b/a)} \left[1 - \log\frac{b}{r} - \frac{a^2}{(b^2-a^2)}\left(1 + \frac{b^2}{r^2}\right)\log\frac{b}{a} \right],$$

$$\sigma_{zz} = \frac{\alpha E T_i}{2(1-\nu)\log(b/a)} \left[1 - 2\log\frac{b}{r} - \frac{2a^2}{(b^2-a^2)}\log\frac{b}{a} \right].$$

Results obtained from the present formulation using GPBEST are compared with the analytical solutions in Fig. 3. The temperature variation (Fig. 3(a)) and the stress variation (Fig. 3(b)) are plotted with respect to the radial distance from the center of the cylinder. As evident, excellent correlation is obtained for all four quantities.

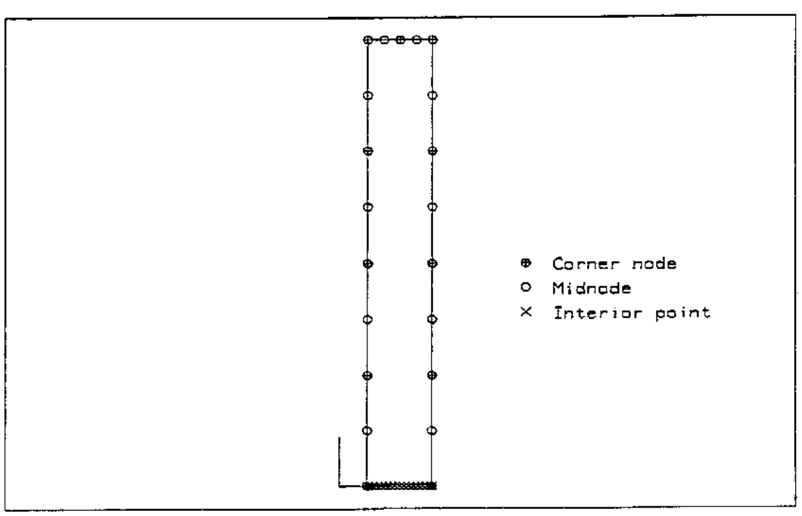

Fig. 2. Cylinder with a circular concentric hole, boundary element model.

5.2. Sudden cooling of a solid cylinder

This example analyzes the response of a long, solid cylinder of radius b with a constant uniform initial temperature of 100 °C whose lateral surface is maintained suddenly at 0 °C temperature. The analytical solution, presented in [18], for the temperature at any given instant t, is given by

$$T = T_0 \sum_{n=1}^{\infty} A_n J_0\left(\beta_n \frac{r}{b}\right) e^{-p_n t},$$

where $J_0(\beta_n(r/b))$ is the Bessel function of order zero and β_n are the roots of the equation $J_0(\beta) = 0$.

In addition, the coefficients of the series, A_n, are

$$A_n = \frac{2}{\beta_n J_1(\beta_n)},$$

and the constants p_n are

$$p_n = \left(\frac{k}{\rho c_\varepsilon}\right)\frac{\beta_n^2}{b^2}.$$

$J_1(\beta_n)$ is the Bessel function of order one and the other symbols have their usual meaning.

The stresses at any instant t and a radius r are given by

$$\sigma_{rr} = \frac{2\alpha E T_0}{(1-\nu)} \sum_{n=1}^{\infty} e^{-p_n t}\left\{\frac{1}{\beta_n^2} - \frac{1}{\beta_n^2}\frac{b}{r}\frac{J_1(\beta_n r/b)}{J_1(\beta_n)}\right\},$$

$$\sigma_{\theta\theta} = \frac{2\alpha E T_0}{(1-\nu)} \sum_{n=1}^{\infty} e^{-p_n t}\left\{\frac{1}{\beta_n^2} + \frac{1}{\beta_n^2}\frac{b}{r}\frac{J_1(\beta_n r/b)}{J_1(\beta_n)} - \frac{J_0(\beta_n r/b)}{\beta_n J_1(\beta_n)}\right\},$$

$$\sigma_{zz} = \frac{2\alpha E T_0}{(1-\nu)} \sum_{n=1}^{\infty} e^{-p_n t}\left\{\frac{2}{\beta_n^2} - \frac{J_0(\beta_n r/b)}{\beta_n J_1(\beta_n)}\right\}.$$

The following material properties are assumed:

$$E = 1.0, \quad \nu = 0.3, \quad \alpha = 1.0, \quad k = 1.0, \quad \rho = 1.0, \quad c_\varepsilon = 1.0.$$

With the above choice of properties, the diffusivity c becomes one. The BEM mesh used for this problem is shown in Fig. 4. It consists of six three-noded boundary elements used to model the cylinder.

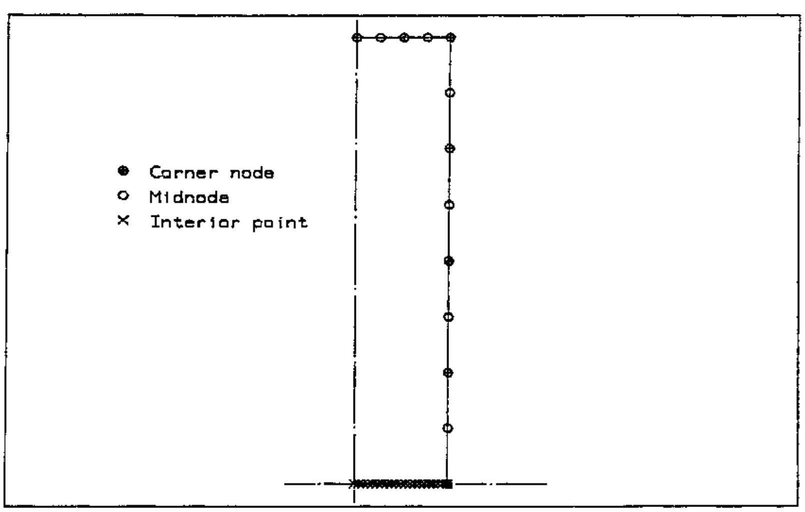

Fig. 4. Cylinder cooled from initial temperature, boundary element model.

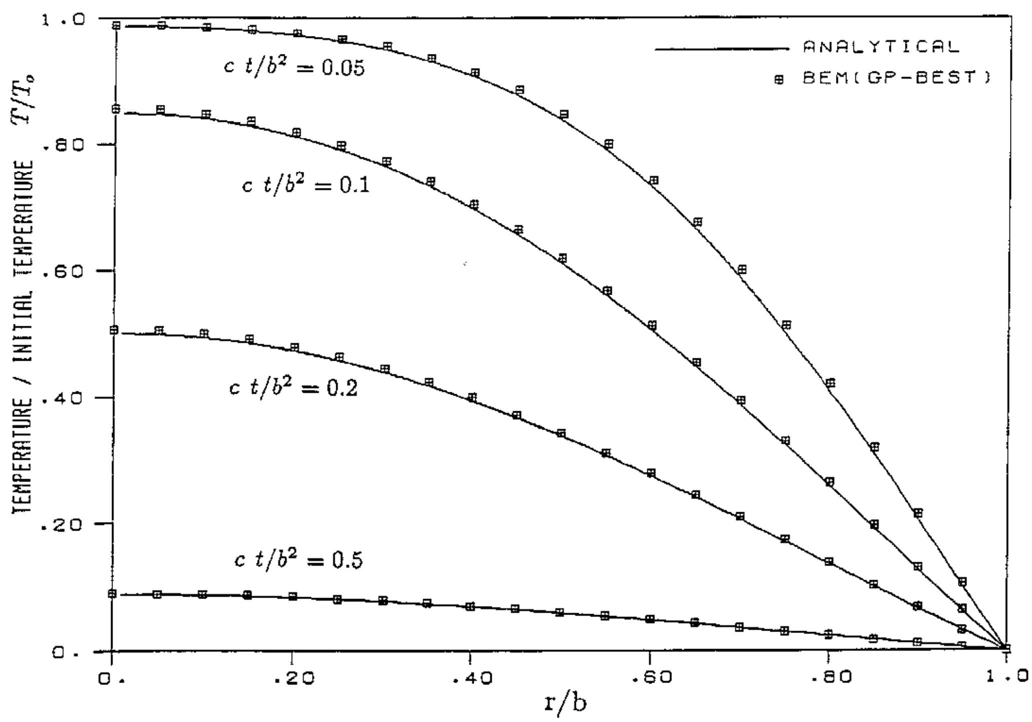

(a)

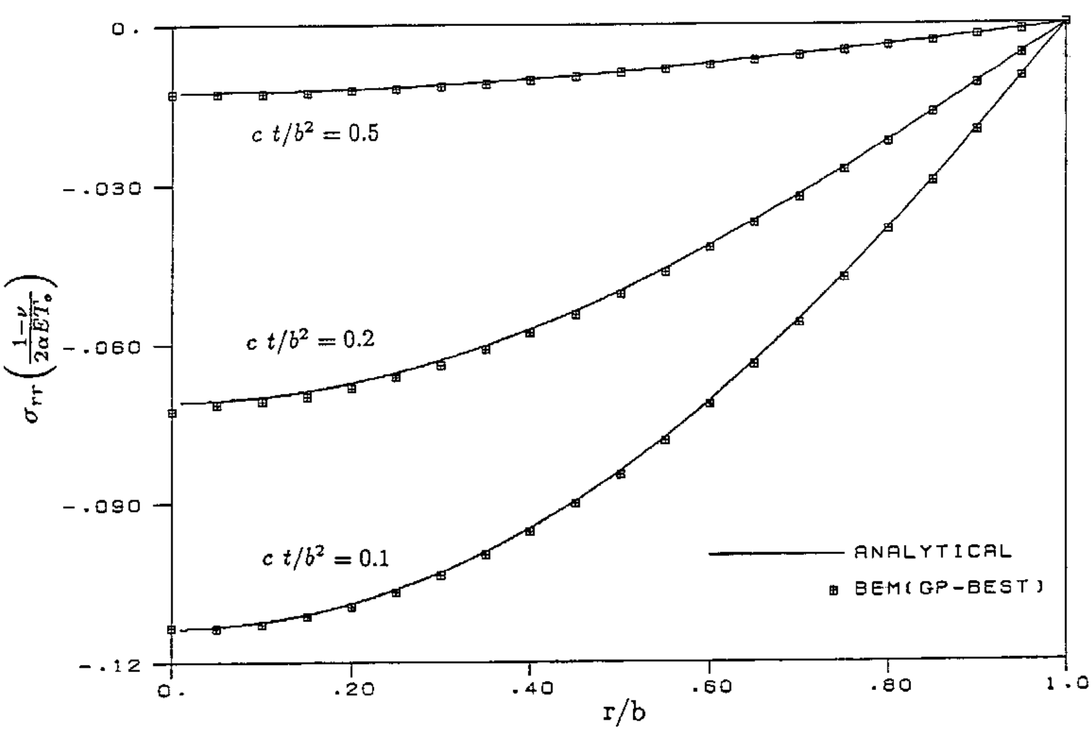

(b)

Fig. 5. (a) Temperature variation along the radius of the cylinder at $ct/b^2 = 0.05$, 0.1, 0.2 and 0.5. (b) Normalized radial stress variation with radial distance for $ct/b^2 = 0.1$, 0.2 and 0.5.

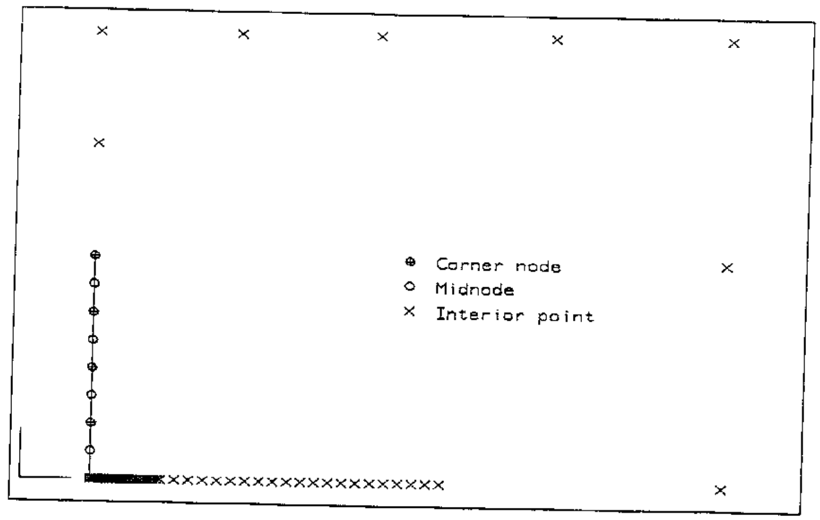

Fig. 7. Heat flow from buried radioactive waste, boundary element model.

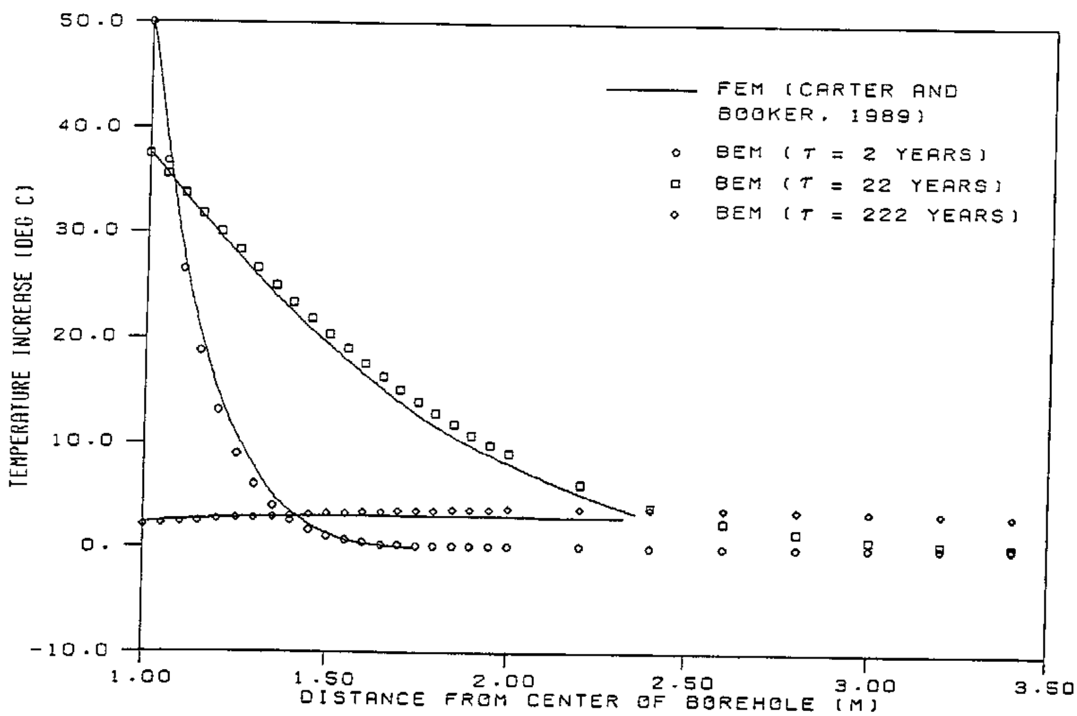

Fig. 8. Temperature increases as a function of distance from the borehole wall for $\tau = 2$, 22 and 222 years.

initial placement. The agreement between the present BEM results and the FEM results is very good for all time values. It may be noted here that the results obtained by Dargush and Banerjee [12] for this problem do not differ from the present BEM results and are, therefore, not displayed. However, the present solution is much more efficient.

Next, in Fig. 9, the results of the radial stress increase in the rock mass due to the waste around the borehole at $\tau = 2$, 22 and 222 years are shown. The stress profile exhibits some differences from the FEM analysis. However, the overall correlation is quite satisfactory in view of the numerical nature of close to the borehole. However, at larger radii away from the wall, the stress change becomes tensile in the circumferential direction. Eventually, all stress changes are only very small as seen by the curve for $\tau = 222$ years. As noted earlier by Dargush and Banerjee [12], the FEM results are shown to be independent of the bore hole radius a, which is not strictly true. Very different responses are obtained for different borehole radii.

6. Conclusions

A linear, axisymmetric time-domain BEM formulation for the evaluation of thermal stresses has been developed in this paper. The present formulation involves only surface variables through the use of infinite space fundamental solutions. Thus, the spatial discretization only requires the modeling of the generator of axisymmetric bodies. The stress integral equations are derived from the corresponding boundary integral equations by differentiation. Starting with the three-dimensional boundary integral formulation, a suitable transformation into a cylindrical coordinate system is conducted. By considering purely axisymmetric loading and boundary conditions, the circumferential degree-of-freedom is removed through integration and the corresponding axisymmetric stress integral equations are developed.

The exact equations are then discretized in time and space using an advanced numerical implementation within a general purpose environment. This allows for the analysis of a number of significant practical applications involving complex geometries and time-dependent boundary conditions. Several such practical problems are studied and very accurate solutions are obtained even for problems with very severe thermal gradients. This provides the basis for establishing the accuracy and effectiveness of the present implementation as a practical analysis tool.

Acknowledgment

The work described in this paper was made possible by a grant from United Technologies Corporation. The authors are indebted to Drs R.B. Wilson and E. Todd of Pratt and Whitney for their support and encouragement.

Appendix A

A.1. Axisymmetric thermoelastic steady-state interior stress kernels

This appendix provides the details of the generalized interior stress kernels for axisymmetric steady-state thermoelasticity. These kernels, when used in conjunction with the numerical tangential integration of the transient part of the three-dimensional kernels in the next section, produce a complete set for quasistatic axisymmetric analysis. The following generalized notation is employed:

$X = x_i = \{R \quad Z\}^{\mathrm{t}}$ coordinates of the integration point or ring source ,

$\xi = \xi_i = \{r \quad z\}^{\mathrm{t}}$ coordinates of the field point ,

$n_r(R, Z)$ normal in the r direction at the integration point ,

$n_z(R, Z)$ normal in the z direction at the integration point .

The indices i, j assume the values 1 and 2 only or, equivalently, r and z. The index T refers to a thermal component in the third position of the generalized displacement or traction vector. Thus, for example, u_T is the temperature while t_T represents the flux. The Greek indices α, β vary from 1 to 3.

The derivatives in the above equations are, in an explicit form,

$$\frac{\partial \hat{G}_{Tr}}{\partial r} = -\frac{M}{r^2 H} a_2 K(m) + \left[\frac{N^2}{r^2 H\rho^2} + \frac{2\bar{Z}^2}{H\rho^2}\right] a_2 E(m) ,$$

$$\frac{\partial \hat{G}_{Tr}}{\partial z} = \left(-\frac{\bar{Z}}{rH}\right) a_2 K(m) + \left(\frac{N\bar{Z}}{rH\rho^2}\right) a_2 E(m) ,$$

$$\frac{\partial \hat{G}_{Tz}}{\partial z} = \left(-\frac{\bar{Z}}{rH}\right) a_2 K(m) + \left(\frac{N\bar{Z}}{rH\rho^2}\right) a_2 E(m) ,$$

$$\frac{\partial \hat{G}_{Tz}}{\partial z} = \left(-\frac{2}{H}\right) a_2 K(m) + \left(\frac{2\bar{Z}^2}{H\rho^2}\right) a_2 E(m)$$

and

$$\begin{aligned}
\frac{\partial \hat{F}_{Tr}}{\partial r} = {} & \left[\left\{-\frac{\bar{Z}}{rRH} - \frac{M\bar{Z}^3}{rRH^3\rho^2}\right\} a_2 k K(m) + \left\{-\frac{\bar{Z}(M+3\bar{Z}^2)}{rRH\rho^2} + \frac{4M^2\bar{Z}^3}{rRH^3\rho^4}\right\} a_2 k E(m)\right] n_r \\
& + \left[\left\{-\frac{1}{rH} + \frac{N\bar{Z}^2}{rH^3\rho^2}\right\} a_2 k K(m) + \left\{\frac{(N+3\bar{Z}^2)}{rH\rho^2} - \frac{4MN\bar{Z}^2}{rH^3\rho^4}\right\} a_2 k E(m)\right] n_z ,
\end{aligned}$$

$$\begin{aligned}
\frac{\partial F_{Tz}}{\partial z} = {} & \left[\left\{\frac{1}{RH} + \frac{\bar{H}\bar{Z}^2}{RH^3\rho^2}\right\} a_2 k K(m) + \left\{\frac{\bar{H} - 3\bar{Z}^2}{RH\rho^2} - \frac{4\bar{H}M\bar{Z}^2}{RH^3\rho^4}\right\} a_2 k E(m)\right] n_r \\
& + \left[\left\{\frac{2\bar{Z}^3}{H^3\rho^2}\right\} a_2 k K(m) + \left\{\frac{6\bar{Z}}{H\rho^2} - \frac{8M\bar{Z}^3}{H^3\rho^4}\right\} a_2 k E(m)\right] n_z ,
\end{aligned}$$

$$\begin{aligned}
\frac{\partial F_{Tr}}{\partial r} = {} & \left[\left\{\frac{2}{RH} - \frac{r^2+R^2}{r^2 RH} - \frac{(r+R)(r^2+R^2)}{rRH^3} - \frac{(r^2+R^2)N}{2r^2 RH^3}\right.\right. \\
& \left. - \frac{MN\bar{Z}^2}{2r^2 RH^3\rho^2} + \frac{HN}{2r^2 RH^2}\right\} a_2 k K(m) \\
& + \left\{\frac{(r^2+R^2)N}{2r^2 RH\rho^2} + \frac{2\bar{Z}^2}{RH\rho^2} - \frac{M\bar{Z}^2}{r^2 RH\rho^2} - \frac{M\bar{Z}^2(R+r)}{rRH^3\rho^2} + \frac{2M\bar{Z}^2(R-r)}{rRH\rho^4}\right. \\
& \left.\left. + \frac{MN\bar{Z}^2}{2r^2 RH^3\rho^2} + \frac{H}{r^2 R} - \frac{(R+r)}{rRH} - \frac{HN}{2r^2 RH^2}\right\} a_2 k E(m)\right] n_r \\
& + \left[\left\{-\frac{3\bar{Z}}{2r^2 h} + \frac{N^2\bar{Z}}{2r^2 H^3\rho^2}\right\} a_2 k K(m) + \left\{\frac{3N\bar{Z}}{2r^2 H\rho^2} + \frac{2\bar{Z}}{H\rho^2} + \frac{N\bar{Z}(R+r)}{rH^3\rho^2}\right.\right. \\
& \left.\left. - \frac{2N\bar{Z}(R-r)}{rH\rho^4} - \frac{N^2\bar{Z}}{2r^2 H^3\rho^2}\right\} a_2 k E(m)\right] n_z ,
\end{aligned}$$

$$\begin{aligned}
\frac{\partial F_{Tz}}{\partial r} = {} & \left[\left\{\frac{\bar{Z}}{rRH} - \frac{M\bar{Z}^3}{rRH^3\rho^2}\right\} a_2 k K(m) + \left\{\frac{-\bar{Z}(N-4r^2)}{2rRH\rho^2} - \frac{\bar{H}\bar{Z}(\rho^2-4r^2)}{2rRH^3\rho^2}\right.\right. \\
& \left.\left. - \frac{2\bar{H}\bar{Z}(R-r)}{RH\rho^4}\right\} a_2 k E(m)\right] n_r \\
& + \left[\left\{-\frac{1}{rH} + \frac{N\bar{Z}^2}{rH^3\rho^2}\right\} a_2 k K(m)\right. \\
& \left. + \left\{\frac{N}{rH\rho^2} - \frac{\bar{Z}^2(\rho^2-4r^2)}{rH^3\rho^2} - \frac{4\bar{Z}^2(R-r)}{H\rho^4}\right\} a_2 k E(m)\right] n_z ,
\end{aligned}$$

$$g_4'(\eta) = \frac{\partial g_4(\eta)}{\partial \eta}$$

and so on.

In the above,

$$\eta = \frac{r}{(c\tau)^{1/2}}, \qquad c = \frac{k}{\rho c_\varepsilon}, \qquad \mathrm{erf}(z) = \frac{2}{\sqrt{\pi}} \int_0^z \mathrm{e}^{-x^2}\,\mathrm{d}x\,,$$

$$h_1(\eta) = \mathrm{erf}\left(\frac{\eta}{2}\right) - \frac{\eta}{\sqrt{\pi}}\,\mathrm{e}^{-\eta^2/4}, \qquad g_4(\eta) = -\mathrm{erf}\left(\frac{\eta}{2}\right) + \frac{2h_1(\eta)}{\eta^2},$$

$$g_5(\eta) = -\mathrm{erf}\left(\frac{\eta}{2}\right), \qquad f_6(\eta) = -\mathrm{erf}\left(\frac{\eta}{2}\right) + \frac{6h_1(\eta)}{\eta^2},$$

$$f_7(\eta) = -\mathrm{erf}\left(\frac{\eta}{2}\right) + \frac{2h_1(\eta)}{\eta^2}, \qquad f_8(\eta) = -h_1(\eta)\,.$$

References

[1] F.J. Rizzo and D.J. Shippy, An advanced boundary integral equation method for three-dimensional thermoelasticity, Internat. J. Numer. Methods Engrg. 11 (1977) 1753–1768.
[2] T.A. Cruse, D.W. Snow and R.B. Wilson, Numerical solutions in axisymmetric elasticity, Comput. & Structures 7 (1977) 445–451.
[3] A.A. Bakr and R.T. Fenner, Boundary integral equation analysis of axisymmetric thermoelastic problems, J. Strain. Anal. 18 (1983) 239–251.
[4] A.A. Bakr, M.J. Abdul Mihsein and R.T. Fenner, Treatment of thermoelastic effects in the axisymmetric boundary integral equation method, J. Thermal Stresses 8 (1985) 291–303.
[5] P.K. Banerjee and R. Butterfield, Boundary Element Methods in Engineering Science (McGraw-Hill, London, 1981).
[6] J. Masinda, Application of the boundary element method to 3D problems of nonstationary thermoelasticity, Engrg. Anal. 1 (1984) 66–69.
[7] M. Tanaka, H. Togoh and M. Kikuta, Boundary element method applied to 2D thermoelastic problems in steady and non-steady states, Engrg. Anal. 1 (1984) 13–19.
[8] S. Sharp and S.L. Crouch, Boundary integral methods for thermoelasticity problems, J. Appl. Mech. 53 (1986) 298–302.
[9] G.F. Dargush and P.K. Banerjee, The boundary element method for plane problems of thermoelasticity, Internat. J. Solids and Structures 25 (1989) 999–1021.
[10] G.F. Dargush and P.K. Banerjee, BEM analysis for three-dimensional problems of transient thermoelasticity, Internat J. Solids and Structures 26 (1990) 199–216.
[11] G.F. Dargush and P.K. Banerjee, A boundary element method for axisymmetric soil consolidation, Internat. J. Solids and Structures 7 (1991) 897–915.
[12] G.F. Dargush and P.K. Banerjee, Time dependent axisymmetric thermoelastic boundary element analysis, Internat. J. Numer. Methods Engrg. 33 (1992) 695–717.
[13] B.A. Boley and J.H. Weiner, Theory of Thermal Stresses (Wiley, New York, 1960).
[14] V. Ionescu-Cazimir, Problem of linear coupled thermoelasticity. Theorems on reciprocity for the dynamic problem of coupled thermoelasticity, I, Bull. Acad. Polonaise Sci., Series Sci Tech. 12 (9) (1964) 473–488.
[15] W. Nowacki, W. Green's functions for a thermoelastic medium (quasistatic problems), Bull. Inst. Polit. Jasi, Sierie Noua 12 (N3–4) (1966) 83–92.
[16] D.P. Henry, D.A. Pape and P.K. Banerjee, New axisymmetric BEM formulation for body forces using particular integrals, ASCE J. Engrg. Mech. 113 (5) (1987) 671–688.
[17] F.J. Rizzo and D.J. Shippy, A formulation and solution procedure for the general non-homogeneous elastic inclusion problems, Internat. J. Solids and Structures 4 (1977) 1161–1179.
[18] S. Timoshenko and J.N. Goodier, Theory of Elasticity, 3rd Edition (McGraw-Hill, New York, 1982).
[19] J.P. Carter and J.R. Booker, Finite element analysis of coupled thermoelasticity, Research Report No. 599, The University of Sydney, Australia, 1989.
[20] S. Ahmad and P.K. Banerjee, Inelastic transient dynamic analysis of three dimensional problems by BEM, Internat. J. Numer. Methods Engrg. 29 (1988) 371–390.